DOE/ER/13007-1
Distribution Category UC-34

Thin-Film Chemical Sensors Based on Electron Tunneling

Final Report

S.K. Khanna
J. Lambe
H.G. LeDuc
A.P. Thakoor

November 15, 1985

Prepared for
U.S. Department of Energy
Through an Agreement with
National Aeronautics and Space Administration
by
Jet Propulsion Laboratory
California Institute of Technology
Pasadena, California

JPL Publication 85-85

DOE/ER/13007-1
Distribution Category UC-34

Thin-Film Chemical Sensors Based on Electron Tunneling

Final Report

S.K. Khanna
J. Lambe
H.G. LeDuc
A.P. Thakoor

November 15, 1985

Prepared for
U.S. Department of Energy
Through an Agreement with
National Aeronautics and Space Administration
by
Jet Propulsion Laboratory
California Institute of Technology
Pasadena, California

JPL Publication 85-85

Prepared by the Jet Propulsion Laboratory, California Institute of Technology, for the U.S. Department of Energy through an agreement with the National Aeronautics and Space Administration.

ABSTRACT

The physical mechanisms underlying a novel chemical sensor based on electron tunneling in metal-insulator-metal (MIM) tunnel junctions were studied. Chemical sensors based on electron tunneling were shown to be sensitive to a variety of substances that include iodine, mercury, bismuth, ethylenedibromide, and ethylenedichloride. A sensitivity of 13 parts per billion of iodine dissolved in hexane was demonstrated. The physical mechanisms involved in the chemical sensitivity of these devices were determined to be the chemical alteration of the surface electronic structure of the top metal electrode in the MIM structure. In addition, electroreflectance spectroscopy (ERS) was studied as a complementary surface-sensitive technique. ERS was shown to be sensitive to both iodine and mercury. Electrolyte electroreflectance and solid-state MIM electroreflectance revealed qualitatively the same chemical response. A modified thin-film structure was also studied in which a chemically active layer was introduced at the top Metal-Insulator interface of the MIM devices. Cobalt phthalocyanine was used for the chemically active layer in this study. Devices modified in this way were shown to be sensitive to iodine and nitrogen dioxide. The chemical sensitivity of the modified structure was due to conductance changes in the active layer.

ACKNOWLEDGMENTS

This work was conducted by the Jet Propulsion Laboratory through NASA Task RE-152, Amendment 345. The Office of Basic Energy Science supported the Project, which was sponsored by DOE/NASA Interagency Agreement No. DE-A101-82ER13007.

CONTENTS

SECTION I

INTRODUCTION

The objective of this study was to investigate the physical mechanisms underlying observed effects in electron tunneling that could form the basis of a chemical sensor. Initial experiments on elastic tunneling in metal-insulator-metal (MIM) thin-film junctions confirmed that the observed tunneling effects are indeed due to surface electronic properties of the metal layers and are, therefore, extremely sensitive to certain specific chemical species to which the junctions are exposed. To develop a complete understanding of the observed tunneling effects, work was initiated in parallel on another, complementary surface-sensitive technique, namely, electroreflectance spectroscopy (ERS). Surface sensitivity of this technique had been demonstrated and promised to provide the complementary information desired. As an added attraction, ERS had the potential of forming the basis of a chemical sensor in its own right. It must be emphasized that a variety of emerging techniques such as inverse photoemission spectroscopy (IPES), electron energy-loss spectroscopy (EELS), angle-resolved photoemission spectroscopy (ARPES), and other sophisticated techniques that probe surface electronic characteristics of solids require elaborate facilities and surface preparation (e.g., ultraclean, ultrahigh vacuum systems, and elaborate in situ sample preparation). In contrast, both EETS and ERS techniques possess extreme surface sensitivity; however, they can still work conveniently under significantly less stringent conditions (e.g., thin-film junctions, once fabricated in situ, can be exposed to ambients with little or no harmful effects). Furthermore, results on these techniques compare well with the rapidly growing literature based on the more sophisticated surface techniques previously listed. A critical comparison of the literature provided a basis for a coherent understanding of observed tunneling effects. In the course of this study a sensitivity of 13 parts per billion (ppb) iodine dissolved in hexane for MIM tunnel junctions was demonstrated.

In addition, the possibility was also explored of modifying the structure of the tunneling devices to enhance their chemical-sensing capabilities. The inclusion of a chemically active layer at the metal-insulator interface of tunneling structures had the potential of achieving this goal. Metal-phthalocyanines [M(PC)] were chosen for study as the active layer because of the large chemical sensitivity of bulk electronic properties of these materials and their chemical stability. The devices produced did not show tunneling behavior; however, extremely sensitive changes in device reactance due to chemical exposure indicated that a sensor of a more conventional nature based on these changes in reactance may be possible in this system. This investigation is of practical interest and is included in this report as a possible area for further study.

This report consists of an introduction (Section I), a discussion of surface-sensitive chemical detection (Section II), and an outline of the investigation of surface-sensitive chemical detection based on EETS and ERS (Sections III and IV). Section V details observations based on studies of structures contained in an active layer of M(PC), Section VI presents the conclusions, and Section VII lists references.

SECTION II

SURFACE-SENSITIVE CHEMICAL DETECTION

It is well known that adsorbates at metal surfaces can alter the surface electronic structure of the host solid (Reference 2-1). In addition, monolayer or submonolayer coverages are often sufficient to produce measurable changes. For this reason the surface electronic structure of metals may be extremely important to ultrasensitive chemical sensing. Surface states are theoretically possible at the truncation of any infinite periodic solid. At such a discontinuity, Bloch wave functions with imaginary wave vector are allowed and under certain conditions can be connected to the external electron wave functions. These states are of interest because, not only are the electrons localized near the surface, but a significant fraction of the quantum mechanical electron charge density actually resides outside the metal surface (Reference 2-2).

This fact has interesting consequences in metals because the surface electrons, unlike the bulk electrons, cannot be screened from external dc fields. Furthermore, because of the rapid screening of fields near the surface, large electric field gradients occur, and surface energy levels can be expected to shift in energy (the linear Stark effect) relative to bulk electronic energy levels.

In recent years, understanding of metal surface electronic structure has increased dramatically. Intrinsic and extrinsic adsorbate induced surface states as well as surface resonances have been observed in a large number of systems by a variety of experimental techniques. Occupied surface states have been observed by Angle-Resolved Photoemission Spectroscopy (References 2-3 through 2-6), Electroreflectance Spectroscopy (Reference 2-7), Electron Energy Loss Spectroscopy (Reference 2-8), and Elastic Electron Tunneling Spectroscopy (Reference 2-9). Unoccupied surface states have been observed by Inverse Photoemission Spectroscopy (References 2-10 through 2-14). Furthermore, contrary to earlier thinking, it has been found that intrinsic surface states and resonances need not be destroyed by adsorbed overlayers but may in some instances retain a large part of their original character. This is in evidence in recent studies of alkali overlayers on metals in which coverage-dependent shifts in the energies of intrinsic surface states were observed (see References 2-4, 2-5, and 2-8). Similar shifts in energies have also been observed for surface resonances, for example, chlorine on copper (see Reference 2-13). This surface sensitivity to adsorbates, combined with two surface-sensitive probes [elastic electron tunneling spectroscopy (EETS) and electroreflectance spectroscopy (ERS)], was used in this study to investigate their potential application in the area of chemical sensing.

PAGE 1-2 INTENTIONALLY BLANK

SECTION III

ELASTIC ELECTRON TUNNELING SPECTROSCOPY

A. BACKGROUND

Elastic electron tunneling spectroscopy (EETS) is directly related to the well-studied (Reference 3-1) inelastic electron tunneling spectroscopy (IETS), which has been used extensively in the observation of vibrational modes in molecules adsorbed at the metal-insulator interface of metal-insulator-metal (MIM) tunnel junctions. IETS is an extremely sensitive technique that produces infrared-like spectra for coverages on the order of a fraction of monolayer (10^{13} molecules/mm^2). In EETS the tremendous sensitivity of tunneling spectroscopy is exploited to probe the electronic structure at the interface of MIM tunnel junctions. In large part, the usefulness of EETS as a surface probe is due to two properties of fcc metals, especially the noble metals. First, fcc metals that are vapor-deposited on amorphous substrates form highly textured films with the (111) crystalographic axis perpendicular to the substrate. Thus, tunneling devices can be made with a well-characterised noble metal plane parallel to the insulating barrier. Second, there is a gap in the bulk electron density of states along the high symmetry (111) direction in the noble metals. In gold this gap extends approximately 4 eV above the Fermi energy and decreases to zero away from the (111) direction. The inability of electrons to propagate along the (111) direction limits the tunneling current due to bulk gold. As a result, weaker electronic structure due to intrinsic or adsorbate induced surface states appearing in this energy range become observable.

It has been demonstrated in this study that EETS is indeed sensitive to both intrinsic (see Reference 2-9) and adsorbate induced/ modified surface states (Reference 3-2). The chemical species studied include iodine, mercury, bismuth, ethylenedibromide (EDB), and ethylenedichloride.

B. EETS EXPERIMENTAL DETAILS

EETS is very similar in experimental details to IETS, which has been reviewed in literature (Reference 3-3). The two spectroscopies differ experimentally in the energy ranges covered. Typically, IETS is limited in energy to the range of energies encompassed by molecular vibrations (<0.5 eV), while EETS is limited in principle only by the breakdown limits of the tunnel junction.

A schematic of metal-insulator-metal junctions is shown in Figure 3-1. Metal M_1 is gold, M_2 is aluminum, and the insulator is aluminum-oxide. The junctions are fabricated in situ in an oil-free, ultrahigh vacuum system (10^{-8} Torr). The base electrode, consisting of an aluminum-strip (0.16 cm wide x ~400 Å thick), is thermally evaporated from a tungsten filament through the appropriate mask onto a glazed ceramic substrate. An oxide layer (~20 Å thick) is grown on the base electrode by plasma-assisted oxidation in a 90% oxygen + 10% water mixture at a total pressure of 100 millitorr. Oxidation times varied from 30 to 60 min. The plasma is maintained by a dc discharge

from a semicircular high-purity aluminum electrode at -500 V relative to the stainless steel vacuum chamber. The noble metal top electrode (0.32 cm wide x ~300 Å thick) is thermally evaporated from a tungsten boat through a mask (under ultrahigh vacuum conditions) onto cooled substrates (~77 K).

One of the attractive features of these junctions is their insensitivity to most elements of a typical laboratory environment. However, junctions exposed to the atmosphere exhibit an increase in resistance with time, presumably due to the gradual thickening of the AlO_x barrier layer by infusion of oxygen and/or moisture from the atmosphere. The rise in junction resistance can be retarded by storing the junctions in a dry box.

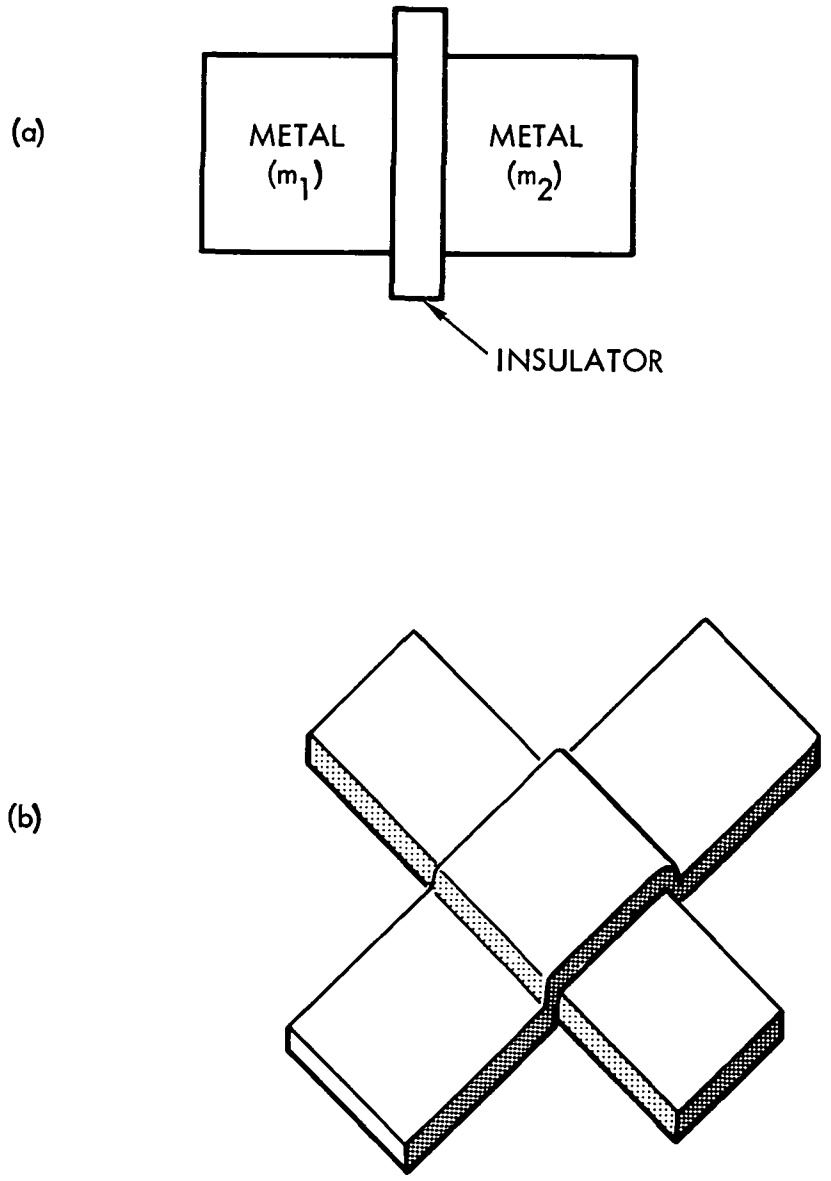

Figure 3-1. Metal-Insulator-Metal (MIM) tunnel junctions (a) schematic and (b) cross geometry

In principle the current-voltage characteristics of the MIM tunnel junctions contain the desired information about the electronic structure of the metals; however, in practice the second derivative of the current with respect to voltage (d^2I/dV^2) is measured to increase sensitivity to small current changes. Figure 3-2 is a schematic of the second derivative tunneling spectrometer used in this study. The second derivative is extracted by applying a small sinusoidal modulation (~10 to 30 mV at 50 KHz) to the dc bias applied to the junction. The component of the potential measured across the junction at the second harmonic of the modulation (100 kHz) is proportional to d^2I/dV^2 and is detected by a synchronous detector. Spectra are obtained by recording d^2I/dV^2 as a function of the dc bias. A signal averager can be added to the spectrometer to improve the signal-to-noise ratio for low-level signals. In this study's experiments the observed signals were large and well above the noise level, allowing the recording of single scans with excellent signal-to-noise ratios.

These junctions were exposed to the detectant by the infusion technique (Reference 3-4). In this technique, completed junctions are exposed to the detectant, which diffuses through the metal top electrode to the active inner surface where it modifies the surface electronic structure. The active surface is at the noble metal-insulator interface and can, to a certain extent, be protected from unwanted contamination from the ambient environment. Exposure can be either from the vapor phase or from solutions containing the detectant.

These junctions were exposed to iodine from solutions of iodine dissolved in either hexane or carbontetrachloride. The infusion process seems to be diffusion-limited, and exposure times were dependent on the molarity of the solution and the gold electrode thickness. For example, for 400 Å thick gold films, exposure times necessary to obtain detectable structure in the spectra varied from 10 s for 10^{-3} molar solutions to 1 h for 10^{-7} molar solutions. Exposure of completed tunnel junctions to mercury vapor at room temperature for 10 min was sufficient to observe useful spectra.

Bismuth exposure was achieved by thermally evaporating ~40 Å of bismuth metal across the gold strips of the completed junctions, followed by heating at 393 K for a few minutes.

C. TUNNELING RESULTS

The initial phase of the tunneling research was concentrated on clean $Al/AlO_x/Au$ junctions. In these studies the goal was to determine what information could be gained about surface electronic structure from tunneling measurements. In the course of this research the first observation of a filled surface state by electron tunneling was made (see Reference 2-9).

Figure 3-3 shows the tunneling spectrum of a clean $Al/AlO_x/Au$ tunnel junction biased with aluminum positive relative to gold. The structure at 0.68 eV is interpreted in terms of a filled surface band on the gold (111) surface, as shown in Figure 3-4. A qualitative understanding of this feature can be otained by examining the schematic of the band structure shown in Figure 3-5. Keeping in mind that the measured quantity is d^2I/dV^2, consider making the gold negative relative to aluminum. The gold is a source

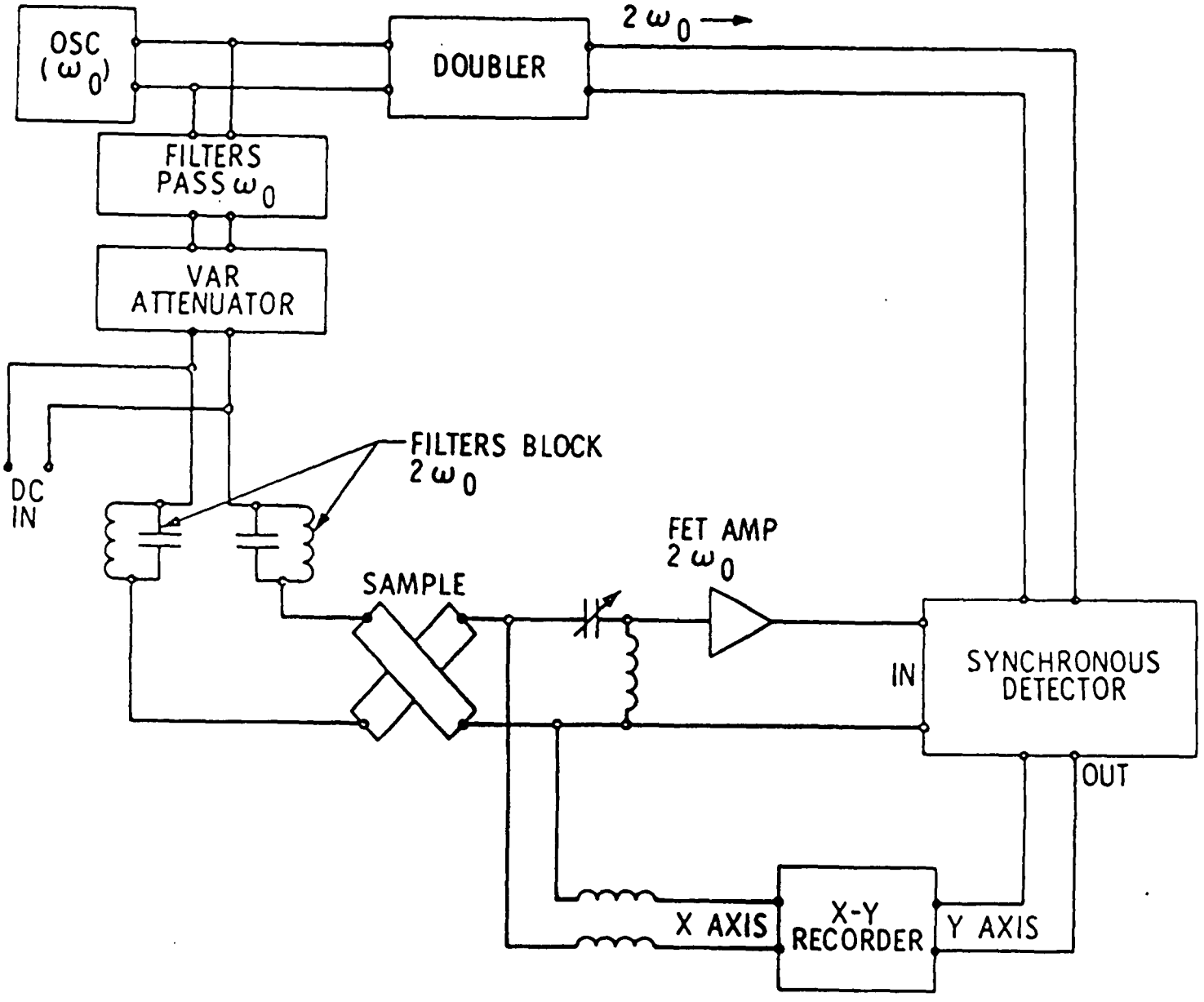

Figure 3-2. Schematic of apparatus used in second-derivative tunneling spectroscopy

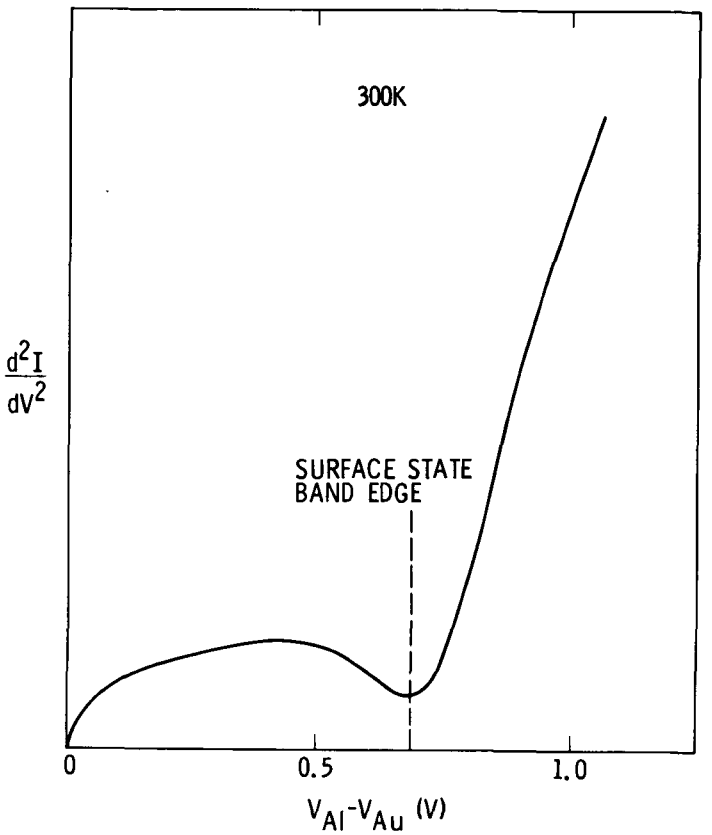

Figure 3-3. Tunneling spectra for $Al/AlO_x/Au$ tunnel junction exhibiting gold surface state. Aluminum is positive relative to gold

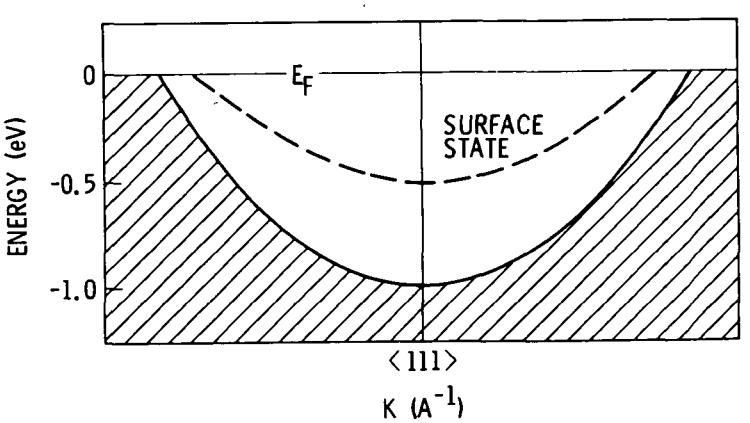

Figure 3-4. Projected surface band structure for the (111) surface of gold exhibiting the calculated position of the surface state relative to bulk states

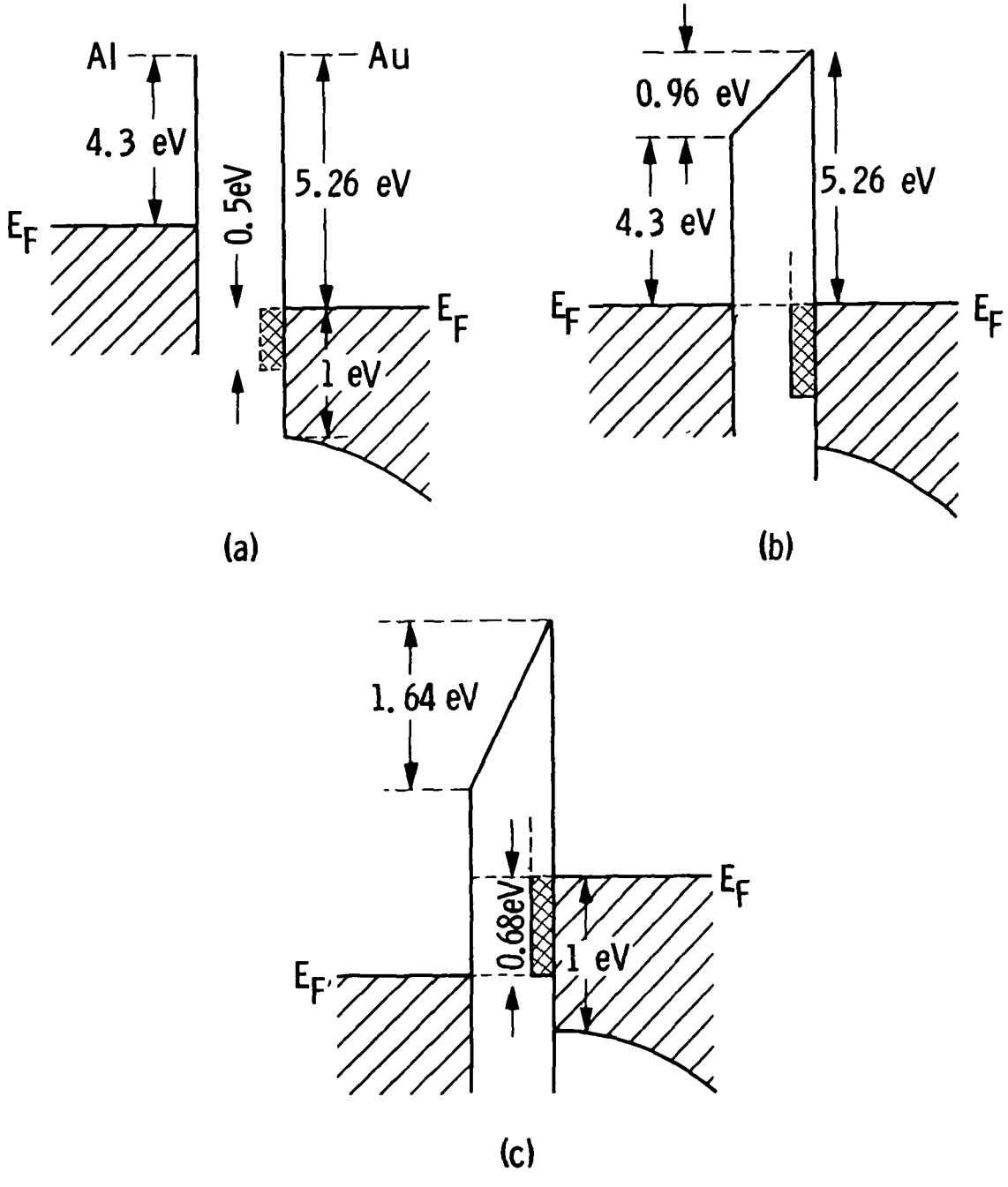

Figure 3-5. Schematic MIM junction showing the gold (111) surface state position relative to the Fermi levels of the two metals as a function of dc bias (a) separated metals (b) junction in equilibrium at zero bias (c) junction biased with Al 0.68 V positive of Au

of electrons that can tunnel into empty states in the aluminum. Specifically, the surface band will contribute to the tunneling current. This contribution will increase with increasing potential until the entire surface band is above the Fermi level in the aluminum, at which point the surface band contribution saturates. This saturation results in the observed minimum of the tunneling spectrum. The shift in energy of the bottom of the surface band, as measured by electron tunneling, can be explained in terms of the linear Stark effect due to the dc bias applied to the junction. The energy of the observed surface state is in good agreement with theoretical calculations (see Reference 2-2) when Stark shifting is taken into account. This result demonstrated that surface electronic structure could be observed by EETS.

A typical tunneling spectra observed after iodine exposure is shown in Figure 3-6. The effects reported are large, involving conductance changes of about 10%. To date these seem to be the largest effects observed by electron tunneling spectroscopy of MIM junctions. The size of the effects are strongly dependent on the quality of the junctions, and thus in situ fabrication of the junctions in a clean, oil-free environment is a necessity. A sensitive quality test of the junctions can be made by observing the tunneling spectra of unexposed junctions with Au positive with respect to Al. For tunneling with this polarity, the occupied Au surface state near the Fermi level appears as a dip in the tunneling spectra at 0.68 eV. The chemically induced structure in the tunneling spectra is strongest for junctions in which the surface state appeared as a strong, well-defined structure and is weak or absent when the surface state structure was weak or absent. This is a strong indication that the effects observed are associated with chemically induced surface features at the Au surface. The dominant structure at 1.8 V varied in energy from approximately 1.7 to 2.1 V from sample to sample. The weaker structure at 2.6 V also varied in energy but followed the lower energy peak, maintaining a 0.7 to 0.8 V difference. The peak positions had a tendency to appear at a somewhat lower energy after the first exposure to iodine and rise in energy upon subsequent exposures. This observation would not be inconsistent with a coverage-dependent shift in an energy level although the infusion method does not give complete control over the amount of iodine actually reaching the interface. Both spectral features could be removed by rinsing the junction in ethanol and heating at approximately 323 K for a few minutes and reappear upon exposure to iodine. It is known that iodine will complex with ethanol, and it is possible that this ethanol rinse will remove iodine from the junction. The lowest concentration solution in which iodine was detected by this method is 10^{-7} molar I_2 in hexane, corresponding to approximately 13-ppb sensitivity. This is an experimental limit due to prohibitive collection times rather than to some intrinsic limit of the detection mechanism. Signals in the 2-V range were also observed for junctions exposed to the organohalides ethylenedibromide (EDB) and dichloroethylene (probably indicating the detection of the halogen in these molecules) and opens up the possibility of the detection of similar organic compounds.

Figure 3-7 shows a spectra obtained for a particularly robust junction in which two additional spectral features are observed at 3.4 and 3.7 V. The higher energy feature at 3.7 V appeared in unexposed junctions and may be associated with an empty surface-state split off from the upper band edge at approximately 4 V.

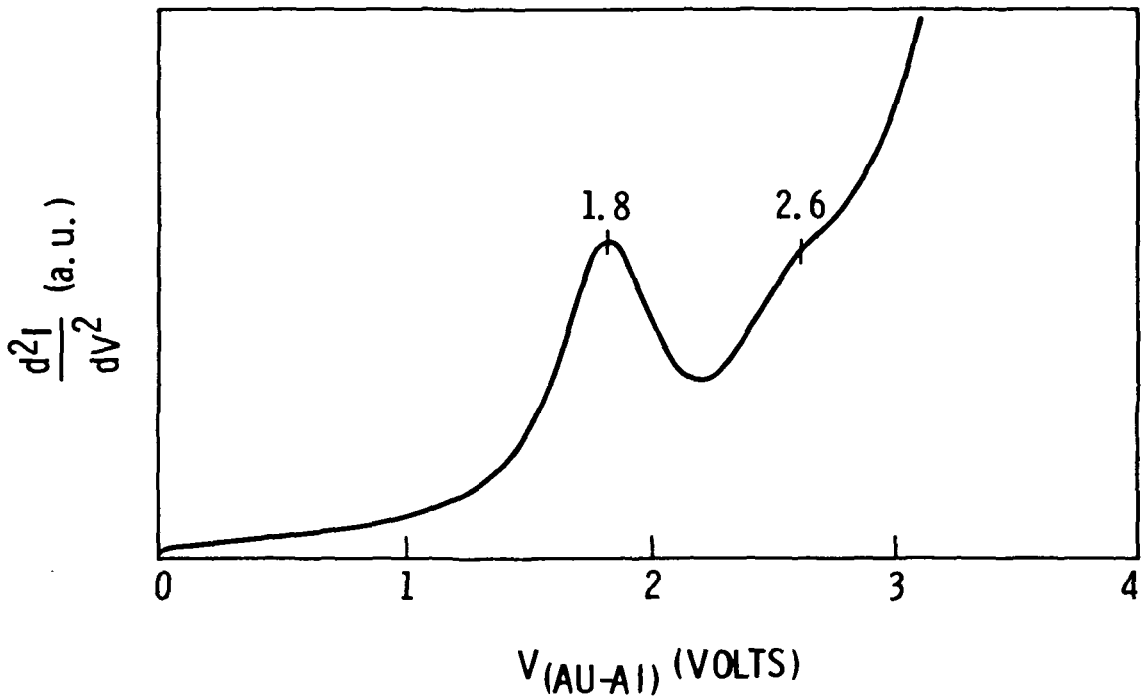

Figure 3-6. Typical tunneling spectra of $Al/AlO_x/Au$ tunnel junctions after exposure to iodine. The vertical axis is in arbitrary units

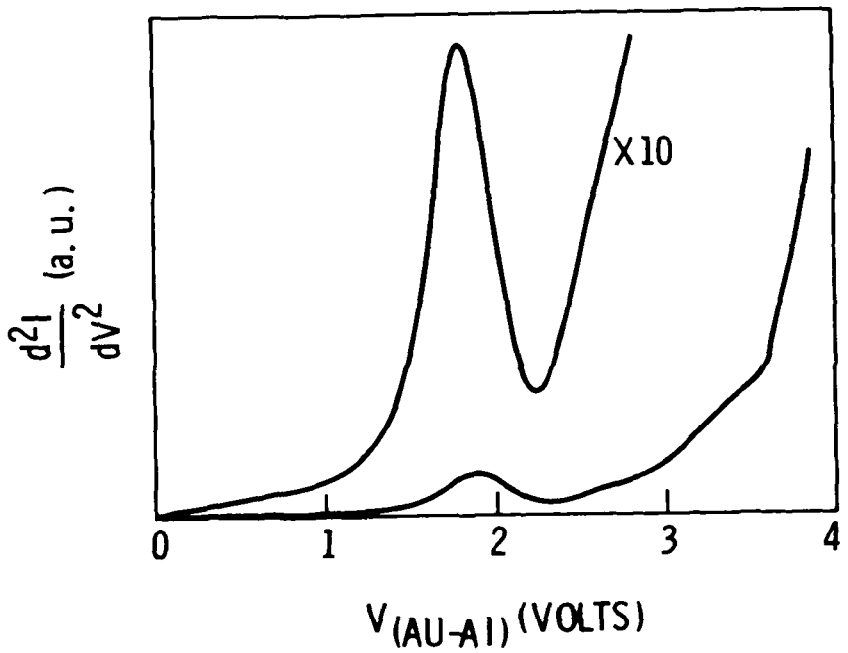

Figure 3-7. Tunneling spectra for robust junction in which higher breakdown voltage allowed scans to ~4 V. These spectra reveal additional structure at higher energies. The vertical axis is in arbitrary units

Spectra observed after mercury and bismuth exposure are shown in Figures 3-8 and 3-9, respectively. The mercury structure at 2.7 V can be removed by heating the junction to 410 K for a few minutes and reappears after exposure to mercury vapor. This process can be repeated many times without degradation of the junction. Exposure times for subsequent exposures are less than that for the initial exposure, indicating that exposure to mercury may increase the porosity of the gold top electrode. The bismuth spectra exhibit a characteristic doublet at 2.5 and 2.8 V.

D. DISCUSSION OF EETS-BASED SENSING

This study shows that Elastic Electron Tunneling Spectroscopy (EETS) is indeed sensitive to the chemical modification due to various detectants. The MIM tunnel junctions do exhibit some limited spectroscopic capabilities and, in the case of iodine and mercury, have been shown to be recyclable. The physical mechanisms underlying the chemical sensitivity of MIM tunnel junctions are now more evident. The structure observed in the tunneling spectra is consistent with the alteration of surface electronic structure due to interaction with the detected species.

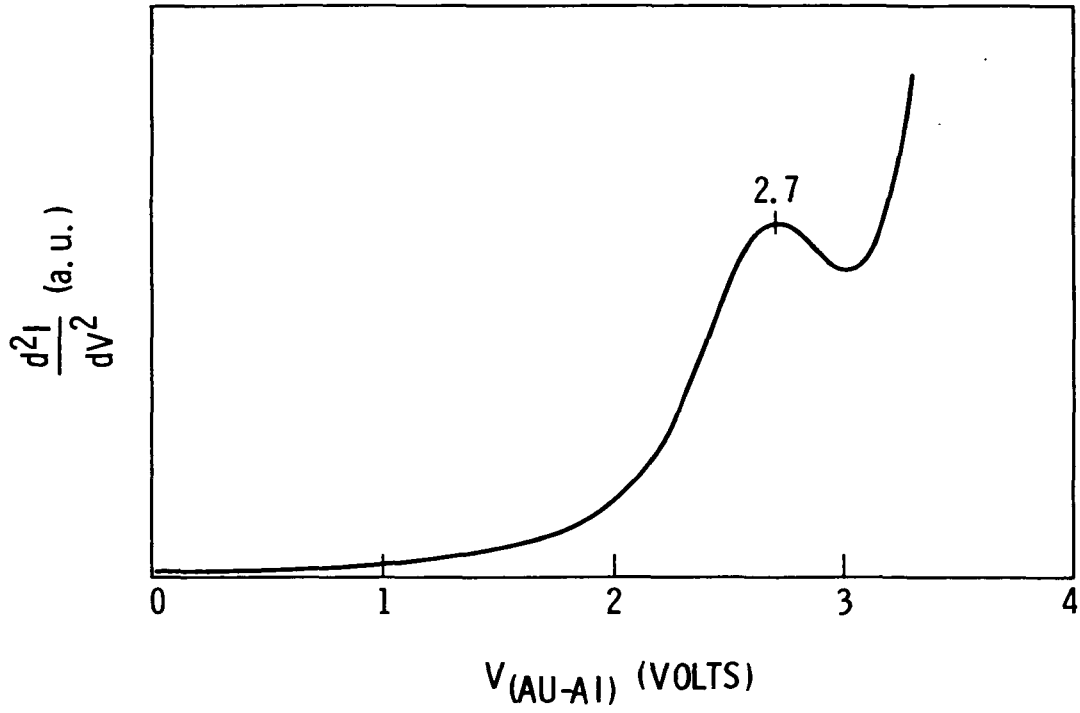

Figure 3-8. Tunneling spectra of $Al/AlO_x/Au$ tunnel junctions after exposure to Hg. The vertical axis is in arbitrary units

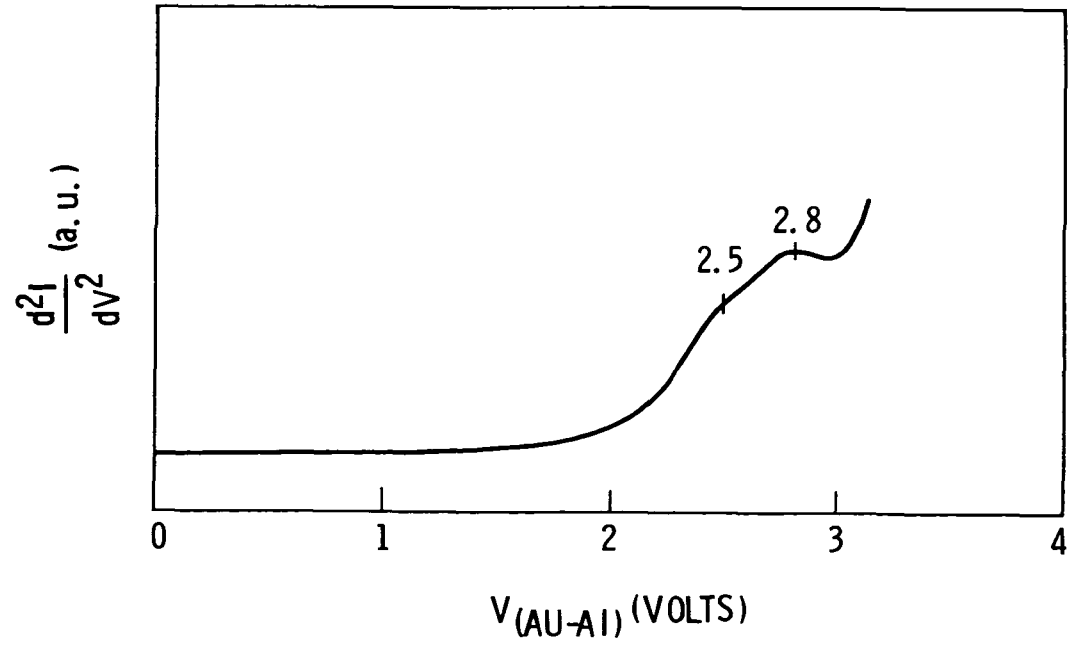

Figure 3-9. Tunneling spectra of $Al/AlO_x/Au$ tunnel junctions exposed to Bi. The vertical axis is in arbitrary units

SECTION IV

ELECTROREFLECTANCE SPECTROSCOPY

A. BACKGROUND

Electroreflectance spectroscopy (ERS) is an experimental technique in which the changes in optical reflectance induced by an external electric field are measured. ERS has been used successfully in the study of bulk band structures in insulators and semiconductors. In metals, dc fields are screened within the first atomic layer of the surface. As a result, ERS in metals is very sensitive to the surface electronic structure and the surface environment. ERS in metals has been plagued by both experimental and interpretational difficulties. However, it has emerged recently as a powerful tool for studying metal surfaces as well as surfaces with adsorbed atoms (References 4-1 and 4-2). This is due, in part, to recent theoretical developments as well as to the availability of improved experimental facilities. Band structure calculations of surface electronic states (see Reference 2-7) have significantly aided in the interpretations of ERS, while the use of clean, well-oriented single crystals have resulted in more reliable and reproducible data.

Of specific interest for this study were the observations of surface states on metal surfaces using ERS (see Reference 2-3). The interpretation of tunneling results as surface states in the present study lead to the conclusion that ERS may be a useful chemical sensing technique.

B. ERS EXPERIMENTAL DETAILS

Figure 4-1 is a schematic of a sample configuration used in electroreflectance. In this configuration the applied fields are perpendicular to the surface of the sample to be studied and are generated by applying a potential between the sample and a transparent electrode. The choice of transparent electrode and dielectric has been the subject of much research (References 4-3 and 4-4). Two approaches to this problem are taken in this study: In the first approach the role of transparent electrode and dielectric are assumed by an electrolyte solution; in the second approach, an MIM sandwich structure is used in which the transparent electrode is a thin (~100 Å), electrically continuous film of metal. In the former configuration the dielectric layer is formed by the depletion region, which naturally forms in the electrolyte near the surface of the sample. For metals in an electrolyte, virtually all of the applied potential is dropped across a thin depletion region (~10 to 20 Å) near the metal surface, producing electric fields on the order of 10^7 V/cm per volt applied. The MIM structure studied consisted of approximately 100 Å of gold deposited on an anodically oxidized aluminum film.

For electrolyte electroreflectance measurements, films of gold ~5000 Å thick were thermally evaporated onto glass substrates in an oil-free, ultrahigh vacuum system. MIM devices were fabricated by first depositing aluminum strips (0.64 cm wide x 1500 Å thick) on glass substrates under high vacuum conditions. An oxide layer was grown on the aluminum by anodization in

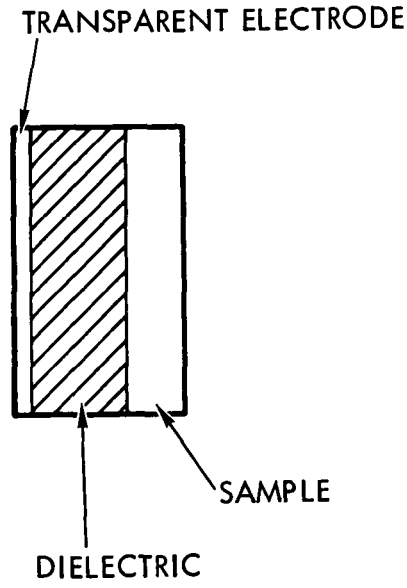

Figure 4-1. Schematic of an electroreflectance cell

an aqueous solution of 3% tartaric acid. Oxide thicknesses varied from 130 to 260 Å, corresponding to anodic potentials of 10 to 20 V. The substrates were returned to the vacuum chamber where gold strips (0.32 cm wide, 100 Å thick) were thermally evaporated across the anodized aluminum strips. The substrates were cooled to 77 K during gold deposition to ensure continuity of the thin gold films.

A schematic diagram of the electroreflectance spectrometer is shown in Figure 4-2. A source of monochromatic radiation was provided by a 150-W xenon dc arc lamp coupled to a Jarrel-Ash 0.25-m monochromator. The mirrors were front-aluminized, spherical mirrors. The detector was a United Detector Technology UV-enhanced silicon photodiode operated in the photovoltaic mode. The modulation potential and frequency were 100 mV-peak square wave at 200 Hz for the electrolyte system and 1.0 V-peak sine wave at 1.0 KHz for the MIM devices. The electrolyte used was 0.5 molar sodium fluoride.

C. ERS RESULTS

Electrolyte electroreflectance spectra for clean and exposed gold surfaces are shown in Figures 4-3 and 4-4 for iodine and mercury exposures, respectively. There are clear effects associated with the chemical exposure in both cases. For mercury, exposure results in a sign change of the ER signal in the visible region whereas for iodine the changes are primarily in the UV. Figures 4-5 and 4-6 show similar spectra for electroreflectance on MIM structures. The spectra taken on MIM structures show the same qualitative behavior as the electrolyte electroreflectance spectra.

D. ERS DISCUSSION

This study indicates that there are easily detectable changes in the electroreflectance signal due to chemical exposure in both the electrolyte ER and solid-state MIM ER. The observed changes are most likely related to changes in surface properties and are not wholly due to electrolyte effect, as

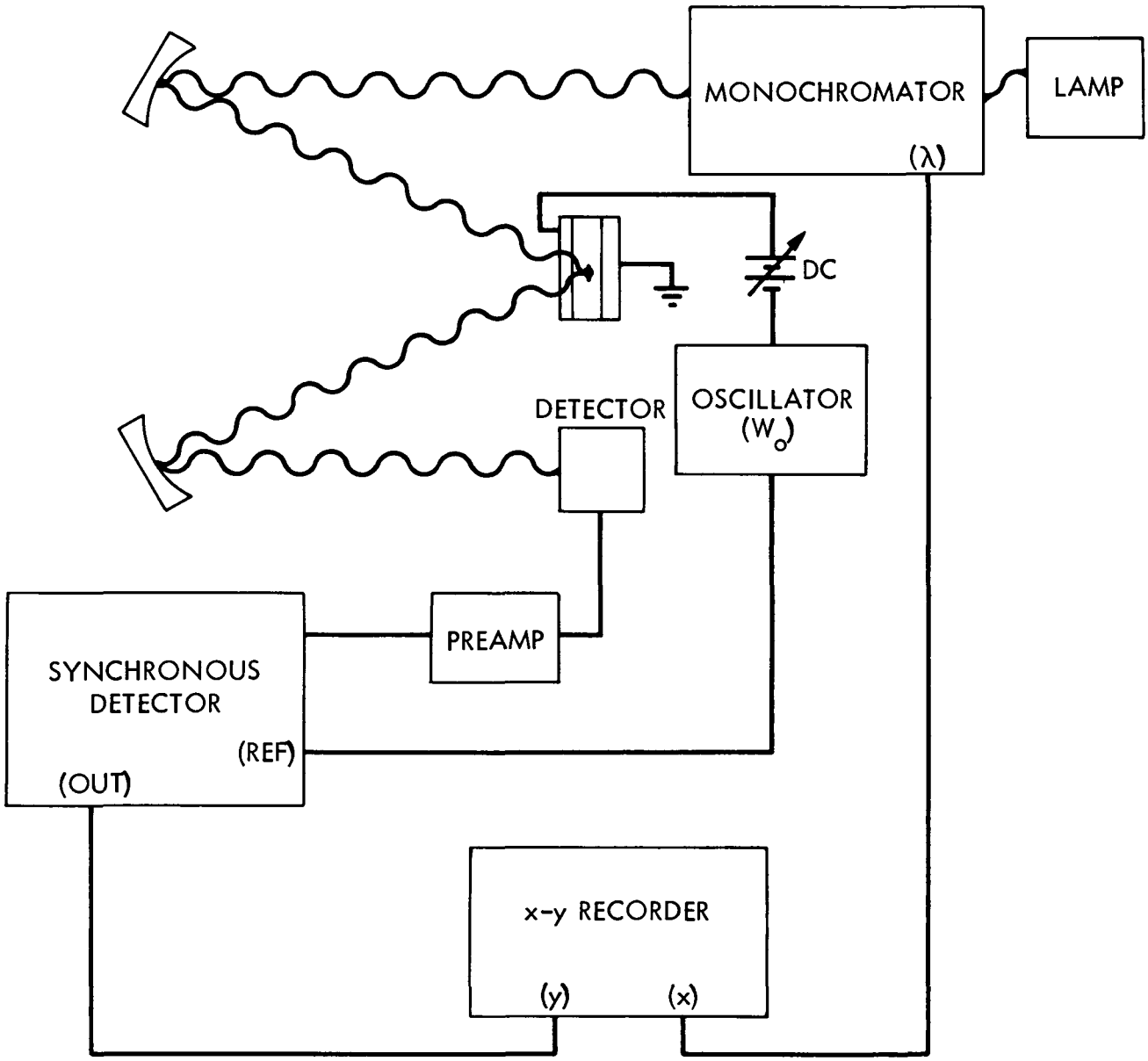

Figure 4-2. Schematic of apparatus for measuring electroreflectance spectra

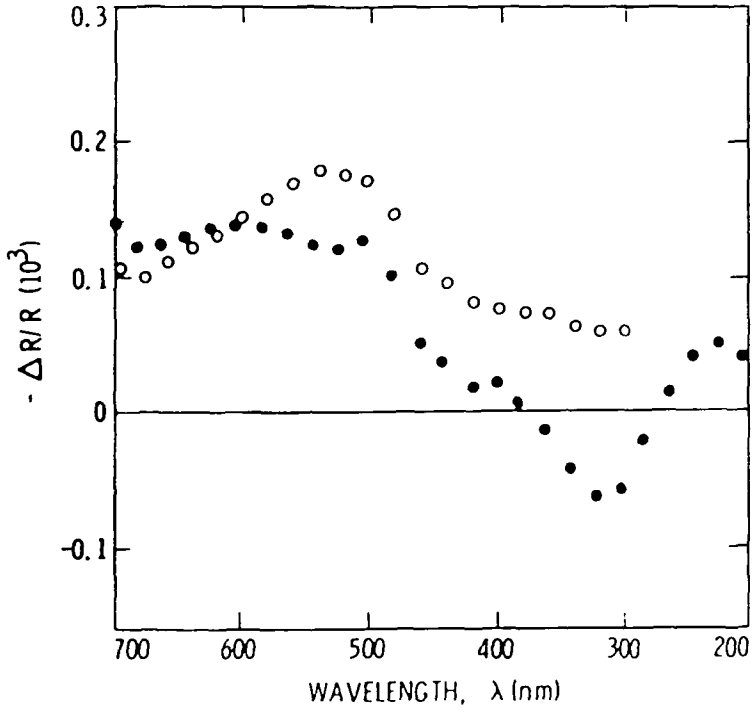

Figure 4-3. Electrolyte electroreflectance of gold before (open circles) and after (closed circles) exposure to iodine

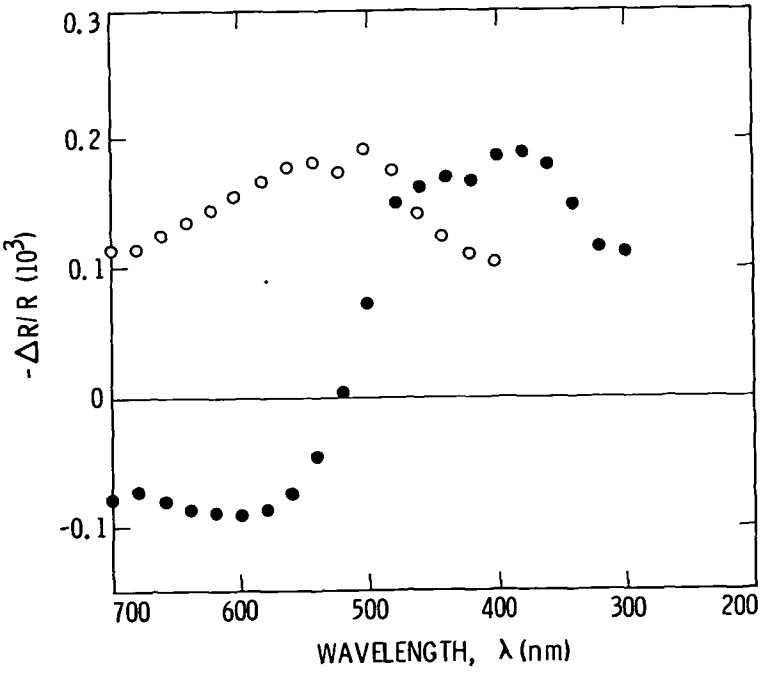

Figure 4-4. Electrolyte electroreflectance of gold before (open circles) and after (closed circles) exposure to mercury

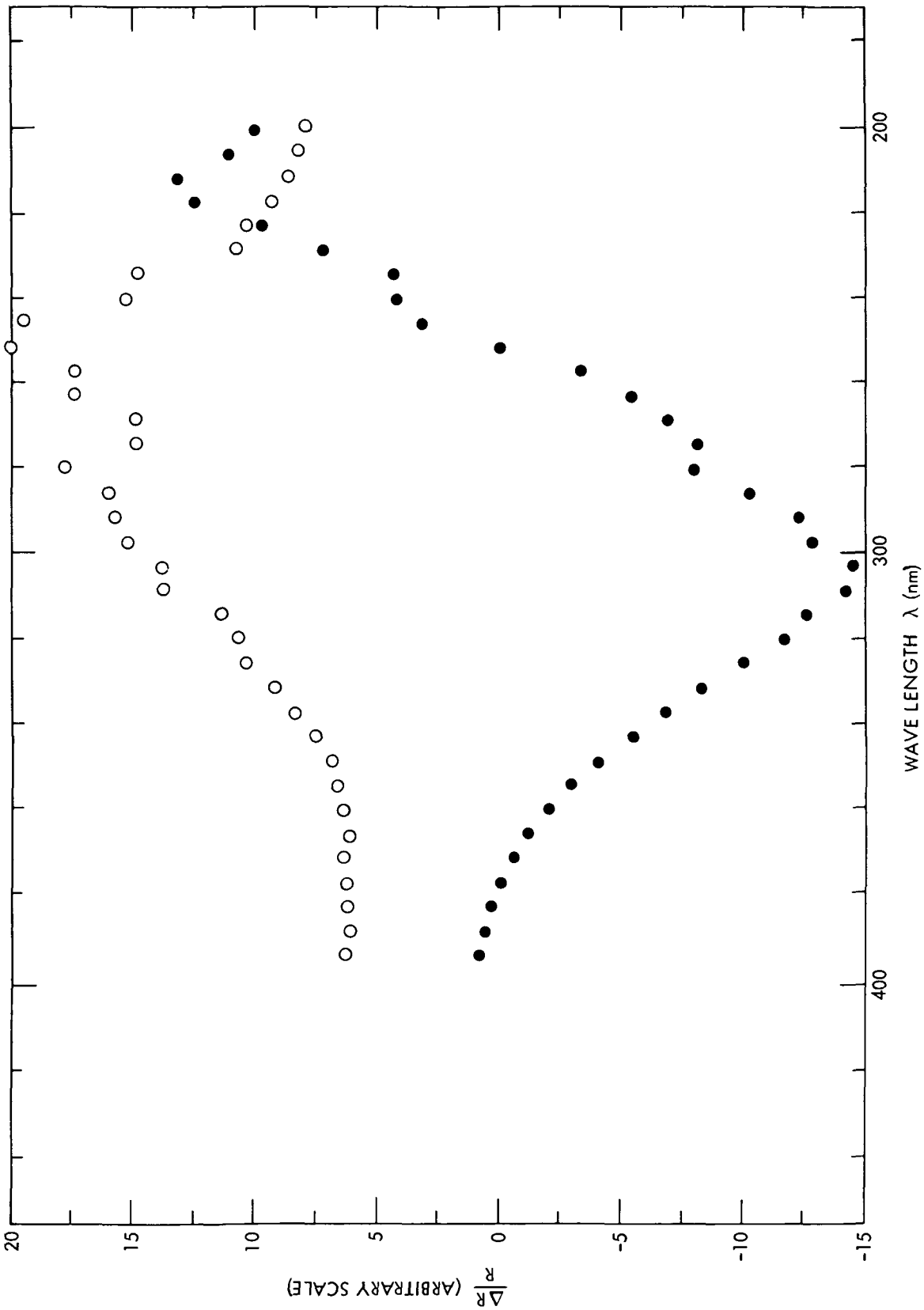

Figure 4-5. Electroreflectance of gold in MIM junctions before (open circles) and after (closed circles) exposure to iodine

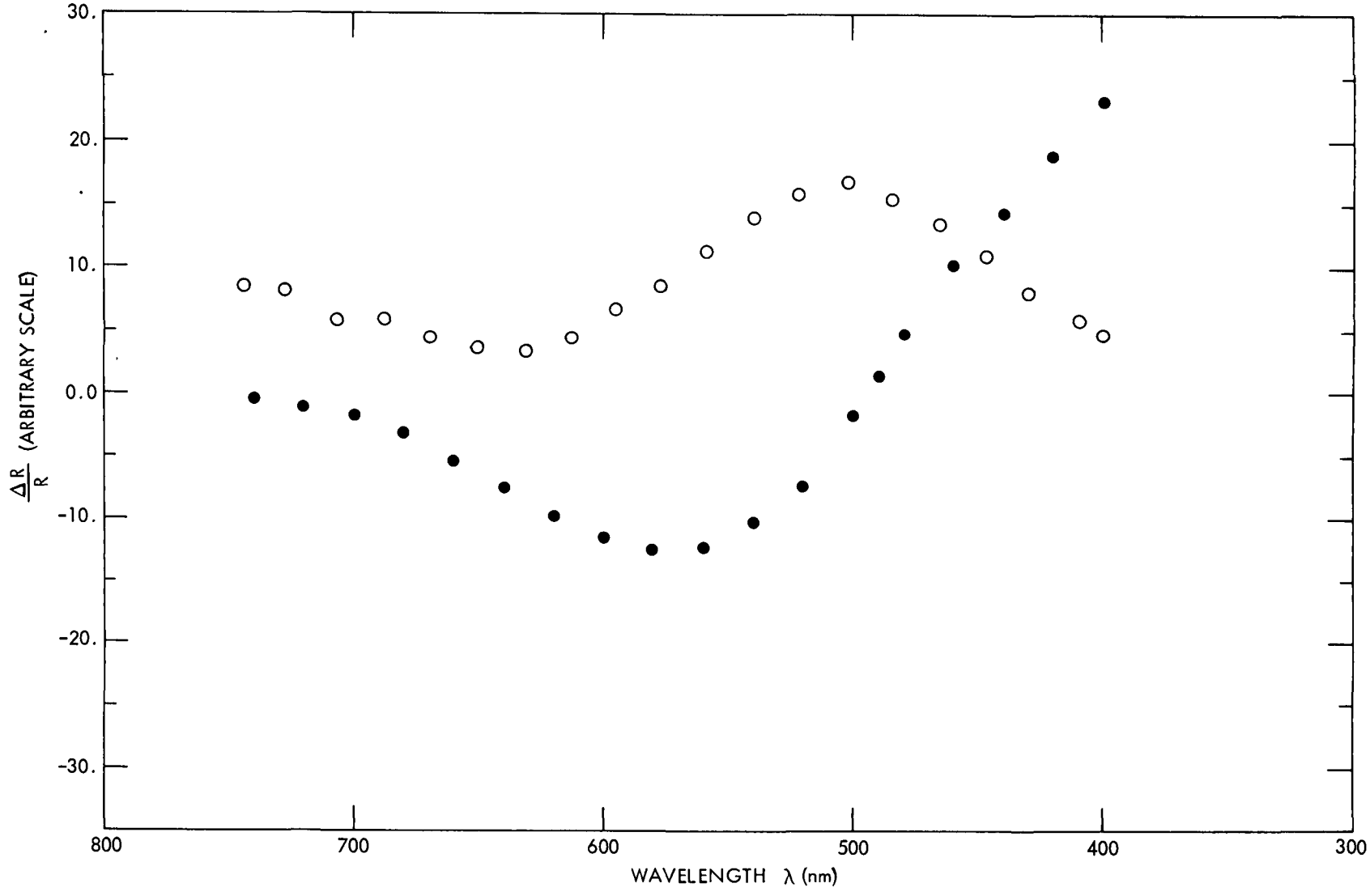

Figure 4-6. Electroreflectance of gold in MIM junctions before (open circles) and after (closed circles) exposure to mercury

indicated by the similarity of MIM and electrolyte results. However, unlike the corresponding tunneling spectra, electroreflectance spectra lack the spectroscopic qualities associated with surface electronic energy levels. In contrast to the quantum effects observed in tunneling, the observed electroreflectance effects may be associated with more general changes in surface properties, such as work-function changes associated with adsorbed layers. If this is the case, detection schemes based on electroreflectance might not have the chemical specificity to be of practical interest. It should be noted that in the case of MIM ER, sensing based on surface states may not be ruled out by the results of this study. Experience with the fabrication of tunnel junction indicates that in situ fabrication under very clean UHV conditions is necessary to observe surface-state effects. Using similar techniques to fabricate MIM devices for ER may lead to the observation of surface-state effects.

SECTION V

CHEMICAL SENSING BASED ON METAL-PHTHALOCYANINES

A. BACKGROUND

There has been much interest recently in sensors based on materials exhibiting large changes in electrical properties due to chemical exposure (Reference 5-1). Of particular interest are a class of robust organic materials, the metal-phthalocyanines M(PC) with M = Ni, Co, Cu, Pb, Fe, and Zn. Pure metal-phthalocyanines are organic solids that are fair insulators with conductivities in the range of 10^{-10} to $10^{-11}\,\Omega^{-1}cm^{-1}$. The conductivity of these materials is very sensitive to impurities that are electronegative enough to oxidize the M(PC) (Reference 5-2). M(PC)s doped with such impurities behave like p-type semiconductors with conductivities approaching 1 to $10\,\Omega^{-1}cm^{-1}$ for large doping densities (References 5-2 through 5-7). An important point to note is that doping can take place by exposing the bulk phthalocyanines to the dopant in the gas or liquid phase. It has been suggested that conductance changes can occur either via surface adsorption of dopants or by incorporation of the dopant in the bulk by solid-state diffusion. The phthalocyanines have open structures that are amenable to diffusion of small atoms or molecules (see Reference 5-3), which may act as electron acceptors creating a hole band. In this way the insulating M(PC) becomes a p-type semiconductor. Alternatively, surface adsorption can alter bulk conductivity by a process in which dopant molecules acquire electrons through surface interactions, creating holes that may be injected into the solid. In either case the bulk (and possibly surface) conductivity change with the addition or removal of dopants from a solid-state system. This is a necessary prerequisite for the chemically active layer in a solid-state electronic sensor. The details of the doping mechanism may have important consequences in terms of the characteristics of actual sensors. Parameters such as sensitivity, response time, and recyclability may depend on the doping mechanisms involved.

Of specific relevance to chemical sensors is the large sensitivity of these materials to nitrogen dioxide (NO_2), a hazardous gas currently in use as an oxidizer for hydrazine in propulsion systems. Recently, a NO_2 sensor based on lead phthalocyanine has been proposed and tested (Reference 5-8). The results are encouraging, with reported sensitivities of 1 ppb to 10 ppm NO_2 in air. The sensor was based on direct conductivity measurements of a 0.3 to 1.0 micron thick film of Pb(PC). In this program a sensor was studied based on a thin-film sandwich configuration of the form: Metal-Insulator-M(PC)-Metal. The insulating layer between the chemically sensitive M(PC) layer and the base electrode allows for thinner active layers while avoiding the disastrous effects of pinholes associated with very thin films.

One can argue that the capacitor configuration chosen has the potential of being faster that the devices based on thicker films. A simple calculation shows that the detector response time should depend on the thickness of the active film, independent of the surface area, in which case thin films would

be better than thick films. The number of detectant molecules collected by the sensor after a given time, t, is proportional to an effective collection volume, V_{eff}:

$$N = c\ V_{eff}(t) \tag{5-1}$$

where

C = dopant concentration in the environment

V_{eff} = effective collection volume

where it has been assumed that all detectants striking the active area stick. For detection from gases or liquids, the effective collection volume as a function of time can be estimated from the mean squared diffusion length in the environment and the effective sensor area:

$$Veff \cong X_{rms} \cdot A_{eff} \simeq \sqrt{2Dt} \cdot A_{eff} \tag{5-2}$$

where the rms diffusion length is approximated by the random walk result and D is the diffusion constant. If one assumes a single charge carrier per dopant molecule collected, the change in carrier density can be approximated by:

$$n = N/V_{active} = N/d\ A_{eff} = c/d\ \sqrt{2Dt} \tag{5-3}$$

where d is the thickness of the active film. Thus, the time required to achieve a given carrier concentration goes down as the thickness of the active layer is decreased. The lower limits to thickness are determined by other considerations, including sensitivity limits of associated electronics and the need for desirable device parameters, such as device impedance.

B. EXPERIMENTAL DETAILS

The devices used in this study consist of multilayered, thin-film structures as shown schematically in Figure 5-1. The fabrication of the $Al/AlO_x/Co(Pc)/Au$ sandwich is similar in many details to the fabrication of tunnel junctions used in this study. The aluminum base electrode (0.16 cm wide x 400 Å thick) is thermally evaporated from a tungsten filament through a mask onto glazed ceramic substrates. The oxide layer is grown by plasma oxidation, as detailed in Section III-B. The ceramic substrate with the oxidized base electrode are transferred to a liquid-nitrogen-trapped, oil-diffusion-pumped vacuum chamber for phthalocyanine deposition. The CO(Pc) layer ~200 to 300 Å thick is thermally sublimed from a tungsten boat at a base pressure of 10^{-6} Torr, rising to 10^{-5} Torr during sublimation. The coated substrates are returned to the oil-free vacuum system where the thin gold top electrode (0.32 cm wide x 100 Å thick) is deposited by thermal evaporation. The substrates are cooled to near 77 K during this operation to ensure the electrical continuity of the gold strips.

The current-voltage characteristics of these devices are dominated by their capacitive reactance. Sensor response was measured by observing the current-voltage characteristics and the harmonic content of the current in these devices as they were exposed to the detectant to be studied. A diagram of the apparatus is shown in Figure 5-2.

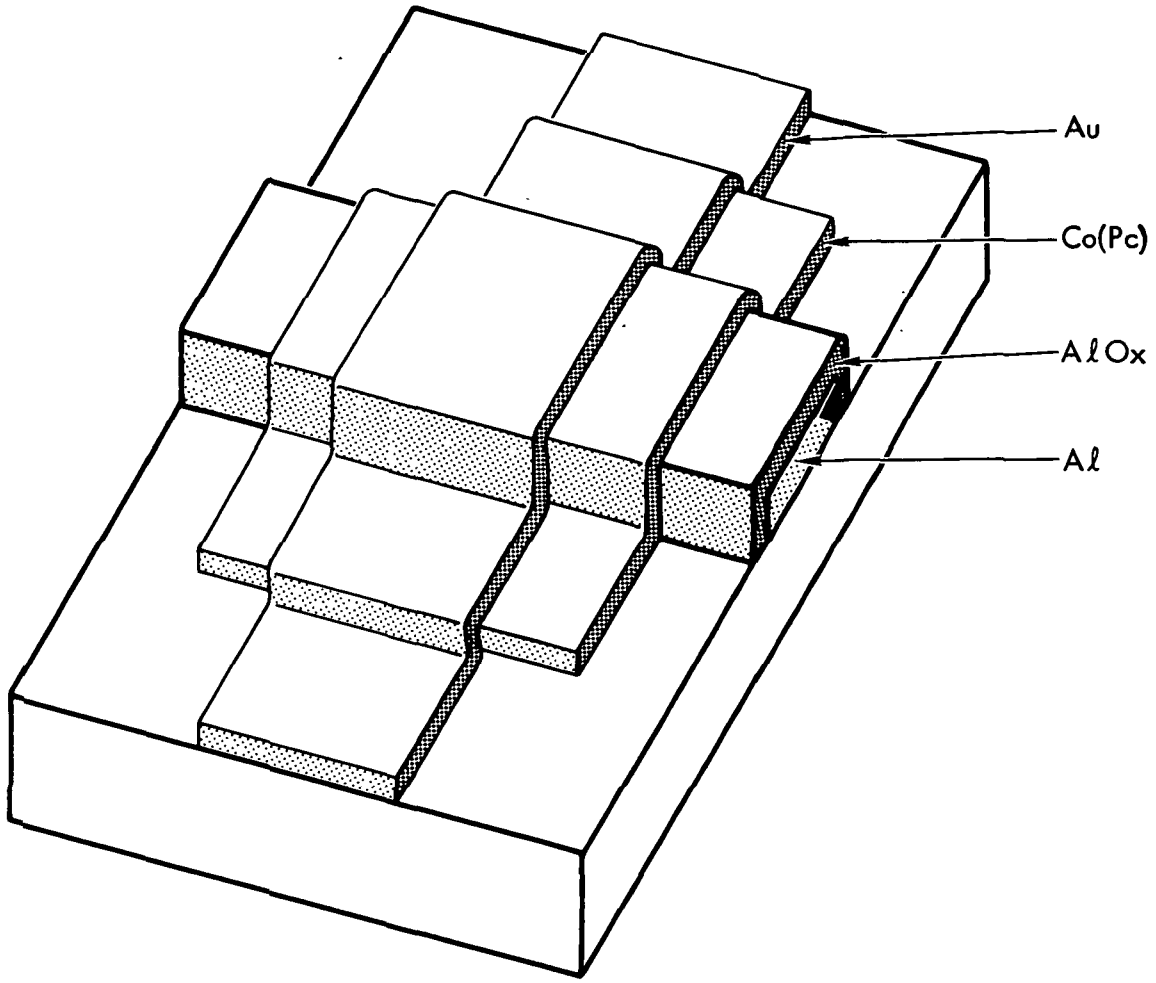

Figure 5-1. Modified thin-film device for chemical sensing based on the chemical sensitivity of cobalt-phthalocyanine [$Co(P_c)$]

The storage oscilloscope is a Nicolet model 2090-III with a model 206 differential input amplifiers and time base. It is used to store current voltage information for before-and-after exposure comparisons. An HP model 3580A spectrum analyser was used to monitor changes in the harmonic content of the current passing through the sensor during exposure. The current response at the fundamental and second harmonic could be monitored as a function of time and exposure level by manually setting the spectrum analyser to those frequencies. The sensors were exposed to iodine by immersing the devices into a vial containing an iodine/hexane solution of the desired concentration. Exposure to nitrogen dioxide (NO_2) is from the gas phase in a mixing chamber containing various concentration NO_2/N_2 mixtures. The mixing chamber is a 1-liter flask, initially purged with dry nitrogen, into which the appropriate amount of NO_2/N_2 is injected by syringe to obtain the desired dilution.

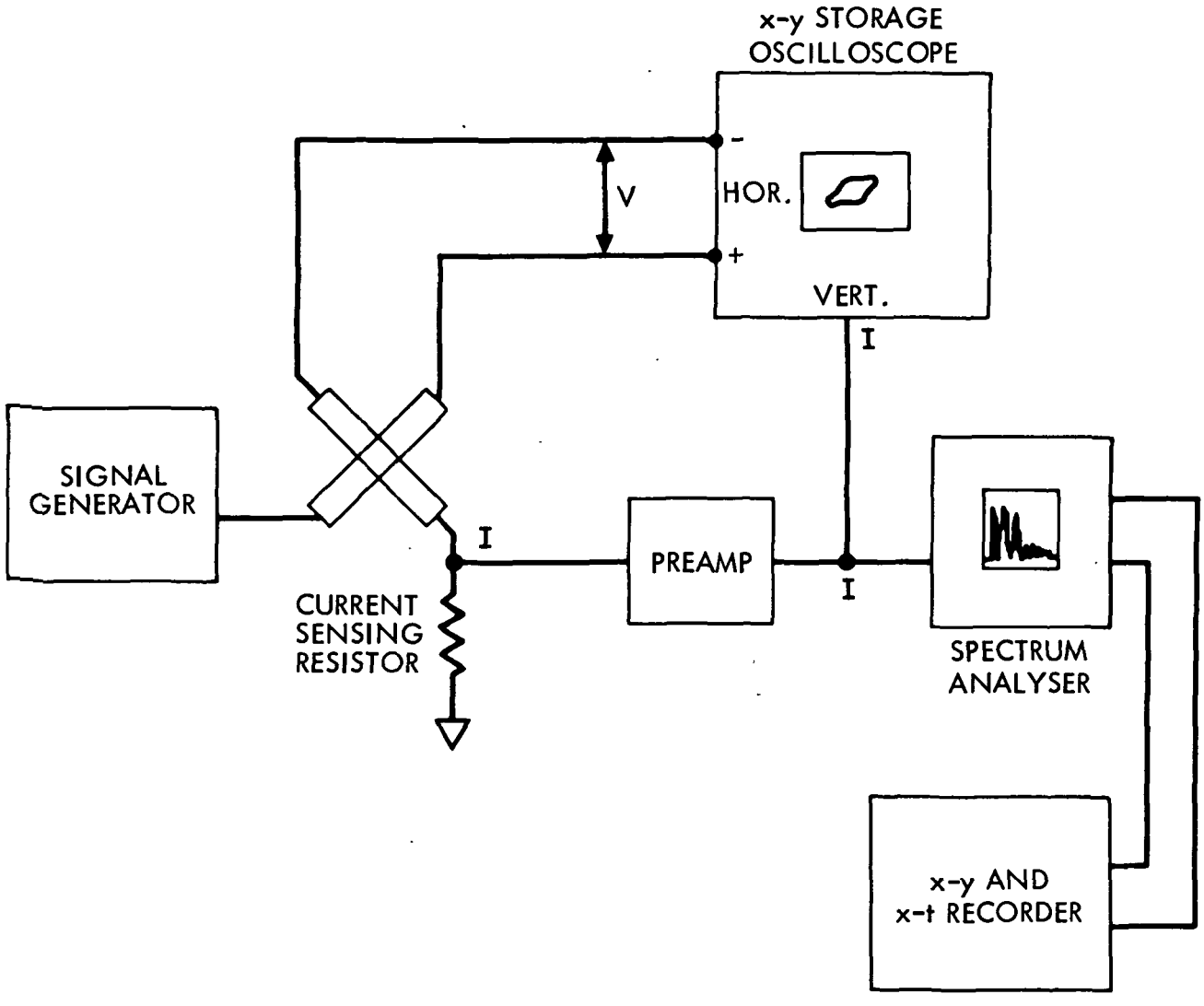

Figure 5-2. Apparatus for measuring I-V character of metal-phthalocyanine thin-film structures

C. RESULTS AND DISCUSSIONS CONCERNING METAL-PHTHALOCYANINES

At the 10-Hz modulation frequency used in these experiments, the current-voltage (I-V) characteristics of the Al/AlO_x/CO(Pc)/Au devices are dominated by the capacitive reactance. The I-V curves are distorted, however, indicating a nonlinear component to the impedance. It is known that a Schottky barrier will form between the metal-phthalocyanines and aluminum (References 5-9 and 5-10) but an Ohmic contact will form at the gold interface. The source of this nonlinearity is the rectifying characteristic of the Schottky barrier. Upon exposure to an acceptor such as iodine or NO_2, the nonlinearity of the device decreases and the capacitive reactance increases. This can be understood in terms of changes in carrier concentration. In essence, the rise in carrier concentration can alter the Schottky barrier characteristics, such as the barrier height and width.

The Schottky barrier can be modeled by a perfect diode shunted by a capacitor. The shunting capacitor depends heavily on the width of the barrier. As the carrier concentration increases, the barrier width decreases and the shunting reactance decreases, thus effectively reducing the bias voltage on the Schottky region which in turn reduces the contribution of the nonlinear component. The overall conductivity of the bulk phthalocyanine also increases so that, with increasing carrier concentration, the impedance becomes increasingly dominated by the Al/AlO_x capacitance.

Exposure to iodine is made from 10^{-3}-10^{-7} molar solutions of iodine in hexane. Freshly made devices exhibit slow response on the first exposure, even to the more concentrated solution. These devices can then be regenerated by a propanol rinse. Their response for subsequent exposures is very fast (on the order of 1 s) even for the lower molarity solutions, indicating that the devices need some presensitization. This effect was also observed in tunneling experiments and can be explained in terms of an increase in the porosity of gold top electrode. This increased porosity manifests itself as an increase in the resistance of the gold arm of the device. For 10^{-7} molar iodine in hexane the response of a sensitized device represents about a 30% increase in current at the modulating frequency, indicating that the sensitivity limits may be much lower than 10^{-7} molar.

An estimate of the upper limit of the number of collected iodine molecules is given by Equation (5-1). For device dimensions, if a typical liquid diffusion constant of 10^{-5} cm^2/s and 1-s exposure time is assumed, for a 10^{-7} molar solution one finds $N \sim 10^{10}$ molecules corresponding to a carrier concentration of 10^{17} carriers/cm^3. This is an upper limit; however, even if it is high by several orders of magnitude, it is clear that significant carrier concentrations can be generated even in dilute solutions.

The response of these devices to NO_2 was carried out with various concentrations of NO_2 in dry nitrogen. Again presensitization by exposure to concentrated solutions and a regeneration with propanol was necessary for optimum response times. The harmonic content of the current as a function of time is shown in Figure 5-3 for an unsensitized junction exposed to 4×10^{-6} molar NO_2 in nitrogen. Figure 5-3 demonstrates the increase in current at the first harmonic and decreases at the second harmonic with increasing time. Such anti-correlation in first and second harmonic behavior may prove important in sensitive sensing strategies. Figure 5-4 shows the relative changes in current at the first and second harmonics as a function of time. For a typical junction exposed to 4×10^{-6} NO_2/N_2 as a function of time, initial responses are on the order of 10 s, and saturation occurs on the order of several minutes. It should be pointed out that the test conditions are not optimum for testing response times because the injected detectant must diffuse through the test chamber before reaching the sample. Response times are probably faster, but these results provide reasonable upper limits. Figure 5-5 shows the relative current changes at the first harmonic as a function of time for various concentrations of detectant. The magnitude of the response depends of the concentration with response times consistently on the order of 1 min, irrespective of concentration. For low concentration exposures the detector can be regenerated by purging the exposure chamber with dry nitrogen. This is a more practical regeneration method in terms of applications than the propanol rinse regeneration.

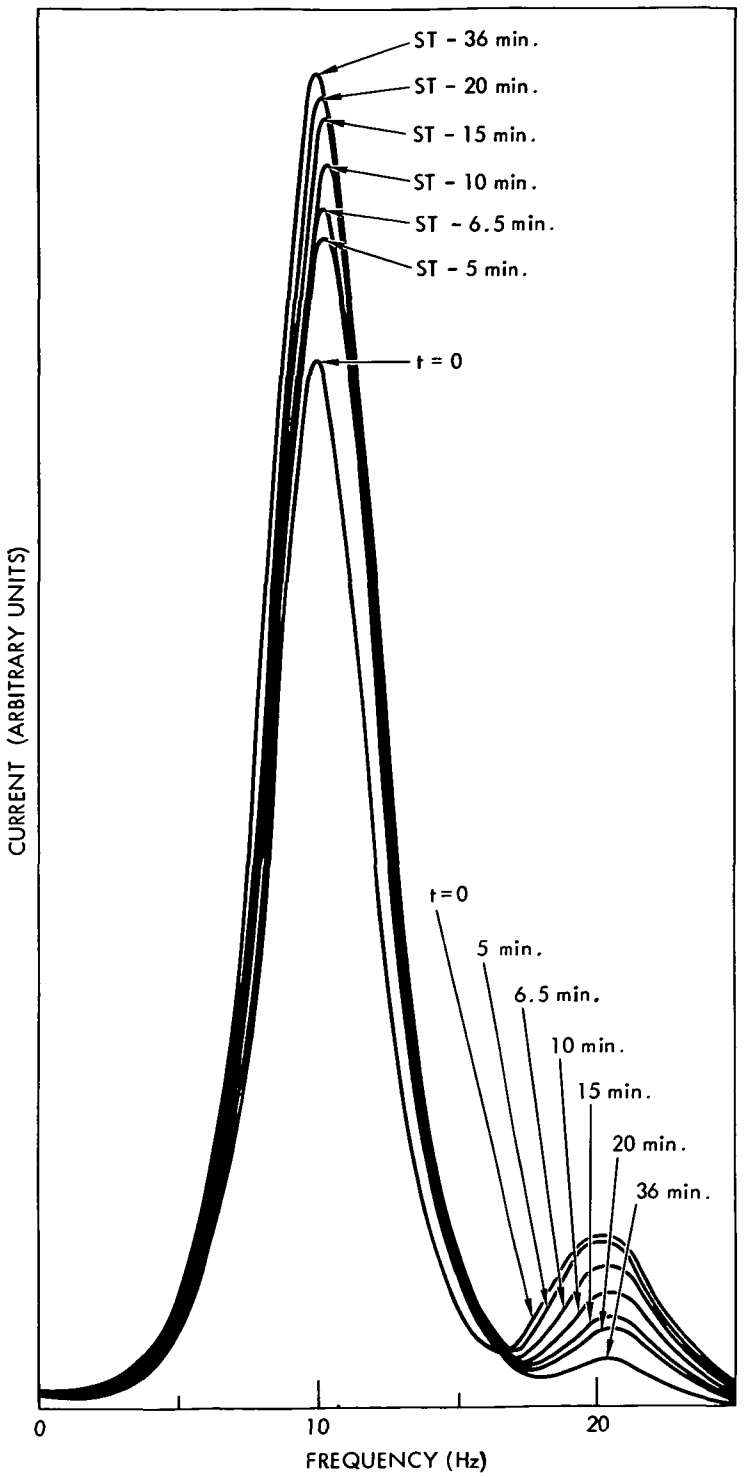

Figure 5-3. Harmonic content of current response as a function of time for Co(Pc) thin-film devices exposed to 4 x 10^{-6} molar NO_2 in nitrogen. Notice the anticorrelation of the responses at the first and second harmonics

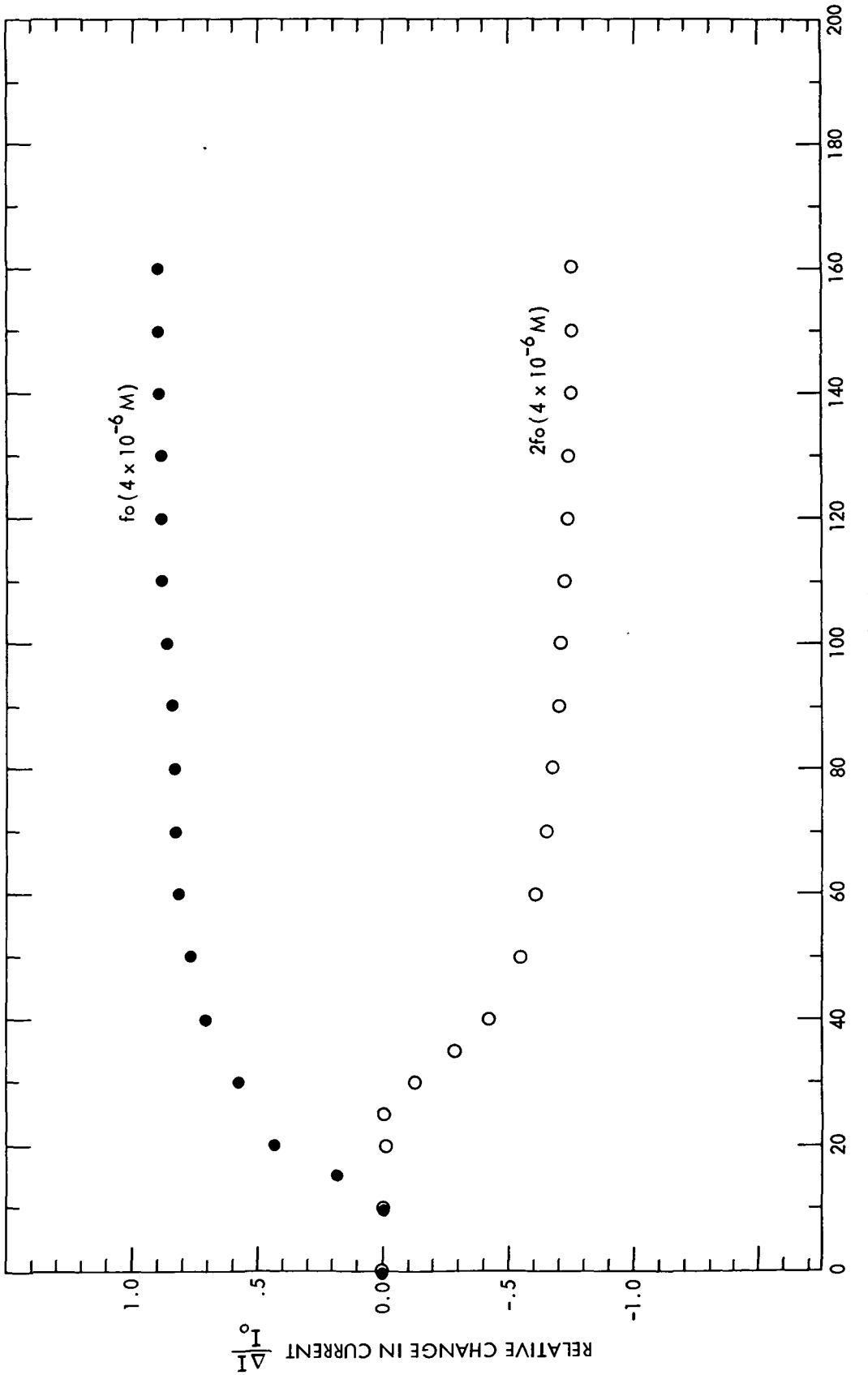

Figure 5-4. Time dependence of the relative current at the first and second harmonics for CO(Pc) to 4×10^{-6} molar NO_2 thin-film devices exposed in nitrogen

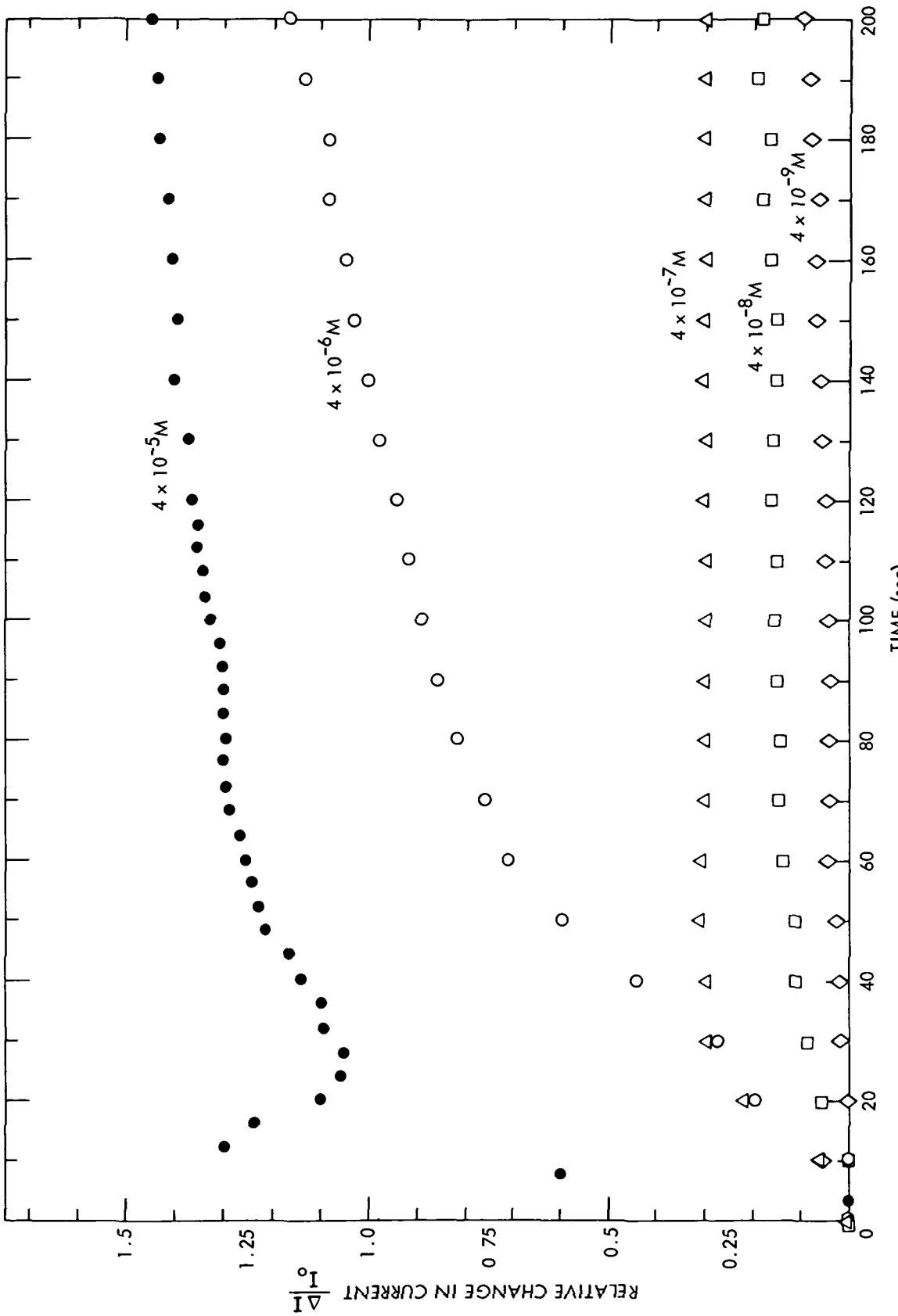

Figure 5-5. Response of Co(Pc) thin-film devices exposed to various concentrations of NO_2 in nitrogen

SECTION VI

CONCLUSIONS

This investigation reports the first observation of a surface state by elastic electron tunneling and indicates that EETS is extremely sensitive to surface electron structure. The study establishes the underlying physical mechanisms responsible for adsorbate-induced structure observed in tunneling spectra of MIM tunnel junctions. Interpretation of this structure in terms of adsorbate induced or altered surface states is consistent with a large body of recent observations by other surface-sensitive techniques. This study demonstrates that chemical species produce characteristic tunneling spectra giving EETS certain specific spectroscopic capabilities and thus the potential for specific chemical detection. The MIM devices are relatively insensitive to the ambient environment but are sensitive to chemical species such as halogens (I, Br), mercury, bismuth, and organohalides (ethylenedibromide, ethylenedichloride) and can be exposed to detectants either in liquids or gasses. The list of detectable species is probably much longer; however, an exhaustive survey of all such species was beyond the scope of the present study. The chemical "signature" of a given chemical species consists of one or a number of modes observed in the tunneling spectra, and the specificity of this technique depends on the ability to distinguish one species signature from another. The study easily distinguishes between the halides, mercury, and bismuth using a combination of mode position and line shape in the tunneling spectra. The halides and organohalides, on the other hand, give very similar spectra, making specific identification difficult. The specificity is limited in these devices because the signature consists of a small number of modes, the mode width can be large, and there is a tendency for modes to shift in position with the magnitude of the exposure.

The latter point, although negative in terms of species identification, may be significantly useful for quantitative determination of species concentration. It must be emphasized that there is a specificity inherent in this technique, which imposes less stringent conditions on "front end" processes such as chemically specific membranes or interactions normally used to enhance specificity. Furthermore, as low as just a monolayer or even a submonolayer coverage (corresponding to $\sim 10^{14}$ molecules/cm^2) is sufficient to produce detectable changes in the surface electronic structure clearly visible in tunneling spectra. The response time of any chemical sensor is dictated by the time necessary to collect the minimum number of the chemical species that can be detected. The collection time is limited by the diffusion of the detectant through the ambient, as indicated by the calculations in Section 5 of this report. In the case of MIM structures the detectant must also diffuse through the metal top layer. Fabrication techniques, such as opening up windows in the top electrode, may minimize the diffusion time. We were able to clearly observe 10^{-7} molar iodine in hexane (corresponding to 13 ppb) using tunneling spectroscopy. MIM structures, although insensitive to most ambients, exhibit a gradual increase in tunneling resistance with time limiting their useful life. Some form of encapsulation is necessary for spot sensors. A more attractive solution may be to develop artificial barriers that do not show their temporal instability. The devices can be purged by heat in the case of mercury and a propanol rinse in the case of iodine.

Investigations on electroreflectance have demonstrated in this study that ERS can sense chemical modification at a metal surface. Both electrolyte and MIM electroreflectance exhibit this chemical sensitivity. The mechanisms underlying the observed effects are not yet clearly understood; however, the effects are reproducible with definite specificity for the two cases studied (I, Hg). Further study on MIM devices is warranted to develop an understanding of the mechanisms involved. If the surface states are involved, the surface sensitivity to chemical species combined with the linear Stark effect (the shifting of energy of electronic states in an applied field) could be used to produce an entirely solid-state, electro-optical chemically sensitive metal surface, and solid-state optical detector combined in a single package comprising a chemical sensor. Readout would occur by electronically sweeping electroreflectance absorption resonances through the fixed laser frequancy using the Stark effect and recording the absorbtion changes versus the applied field.

Investigation of metal-phthalocyanines in this study demonstrated that thin-film structures of this type are chemically sensitive and have the potential for fast response times. The response of $Al/AlO_x/Co(Pc)/Au$ devices to iodine and nitrogen dioxide was studied. Responses were obtained to 10^{-7} molar iodine in hexane and to as low as 10^{-9} molar nitrogen dioxide in nitrogen. In the case of NO_2, the initial response is fast, in seconds after exposure and saturation in minutes. Furthermore, the response time is independent of detectant concentration to a large extent. The magnitude of the response is primarily dependent of the detectant concentration, making quantitative detectors based on these devices possible. The change in impedance nonlinearity of these devices associated with chemical exposure may be useful in electronic readout of these devices. The anticorrelation between the current response at the first and second harmonics due to the change in linearity may be used to decrease sensitivity to drift. The devices will respond to a variety of chemical species that can dope the phthalocyanine layer (this includes a wide variety of chemical species generally considered as good acceptors). Some specificity within this group of detectants can be obtained from the magnitude of the detector response as the conductivities can change by orders of magnitude between equal quantities of different dopants. This would not be acceptable in a detector of low levels of detectant because the magnitude of response depends on detectant concentration as well as on chemical species. Again, specificity in a practical sensor will most likely rely on extrinsically imposed specificity (ion-specific membranes, for example, or on the use of multiple sensors and correlating their responses). These devices could be purged with propanol, and for low-level NO_2 concentrations, by a nitrogen gas purge.

SECTION VII

REFERENCES

2-1. For example, see Morrison, S. R., The Chemical Physics of Surfaces, Plenum Press, New York, 1977.

2-2. Ho, K. M., Harmon, B. N., and Liu, S. H., "Surface-State Contribution to the Electroreflectance of Noble Metals," Phys. Rev. Lett., Vol. 44, No. 23, p. 1531, June 9, 1980.

2-3. Hussain, Z., and Smith, N. V., "Determination of the E(k) Relation for a Surface State on Au(111)," Phys. Rev. Lett., Vol. 66A, No. 6, pp. 492-4, June 26, 1978.

2-4. Lindgren, S. A., and Wallden, L., "Cu Surface State and Cs Valence Electrons in Photoelectron Spectra from the Cu(111)/Cs Adsorption System," Solid State Commun., Vol. 28, pp. 283-286, 1978. Pergamon Press Ltd. Printed in Great Britain.

2-5. Lindgren, S. A., and Wallden, L., "Photoemission of Electrons at the Cu(111)/Na Interface," Solid State Commun., Vol. 34, pp. 671-673, 1980.

2-6. Blanchet, G. B., Dinardo, N. J., and Plummer, E. W., "H on Tungsten (110): Studied by Angle Resolved Photoemission and Inelastic Electron Scattering," Surf. Sci., Vol. 118, No. 3, pp. 496-512, June, 1982.

2-7. Kolb, D. M., Boeck, W., Ho, K. M., and Liu, S. H., "Observation of Surface States on Ag(100) by Infrared and Visible Electroreflectance Spectroscopy," Phys. Rev. Lett., Vol. 47, No. 26, p. 1921, December 28, 1981.

2-8. Soukiassian, P., Riwan, R., Guillot, C., Lecante, J., and Borensztein, Y., "Electron Spectroscopy on Adsorption of Cs on Transition Metals," Phys. Scr., Vol. T4, pp. 110-12, 1983.

2-9. Lambe, J., Thakoor, A. P., and Khanna, S. K., "Observation of Surface States on Gold Films by Electron Tunneling Spectroscopy," J. Vac. Sci. Tech., Vol. 2, pp. 792-4, June 1984.

2-10. Reihl, B., Schlittler, R. R., and Neff, H., "Unoccupied Surface State on Ag(110) as Revealed by Inverse Photoemission," Phys. Rev. Lett., Vol. 52, No. 20, p. 1926, May 14, 1984.

2-11. Himpsel, F. J., and Fauster, T., "Empty Orbitals of Adsorbates Determined by Inverse Ultraviolet Photoemission," Phys. Rev. Lett., Vol. 49, No. 21, p. 1583, November 22, 1982.

2-12. Fauster, T., and Himpsel, F. J., "2π-derived States for CO on Ni(111) Studied by Bremsstrahlung Spectroscopy," Phys. Rev. B, Vol. 27, No. 2, pp. 1390-3, January 15, 1983.

2-13. Dose, V., Altmann, W., Goldmann, A., Kolac, U., and Rogozik, J., "Image-Potential States Observed by Inverse Photoemission," Phys. Rev. Lett., Vol. 52, No. 21, p. 1919, May 21, 1984.

2-14. Reihl, B., Frank, K. H., and Schlittler, R. R., "Image-potential and Intrinsic Surface States on Ag(100)," Phys. Rev. B, Vol. 30, No. 12, pp. 7328-31, December 15, 1984.

3-1. Khanna, S. K., and Lambe, J., "Inelastic Electron Tunneling Spectroscopy," Science, Vol. 220, pp. 1345-1351, 1983.

3-2. LeDuc, H. G., Lambe, J., Thakoor, A. P., and Khanna, S. K., to be published (tentatively J. Appl. Phys.).

3-3. An excellent review of IETS is given in Tunneling Spectroscopy, P. K. Hansma, (ed.), Plenum Press, New York, 1982.

3-4. Jaklevic, R. C., "Infusion Doping of Tunnel Junctions," in Tunneling Spectroscopy, Plenum Press, New York, 1982.

4-1. Kolb, D. M., and McIntyre, J. D., "Electrochemical Modulation Spectroscopy," Sur. Sci, Vol. 37, p. 658, 1973.

4-2. Kolb, D. M., Leutloff, D., and Przasnyski M., "Optical Properties of Gold Electrode Surfaces Covered with Metal Monolayers," Sur. Sci., Vol. 47, No. 22, pp. 622-34, February 1975.

4-3. Cardona, M., Modulation Spectroscopy, Academic Press, New York, 1969.

4-4. Seraphin, B. O., "Electroreflectance," in Semiconductors and Semimetals, ed. R.K. Willardson and A. Beer, Vol. 9, Academic Press, New York, 1972.

5-1. Zemac, J. N., Keramati, B., Spivak, C. W., and D'Amico, A., "Non-FET Chemical Sensors," Sensors and Actuators, Vol. 1, p. 427, 1981.

5-2. Peterson, J. C., Schramm, C. S., Stojakoyic, D. R., Hoffman, B. M., and Marks, T. J., "A New Class of Highly Conductive Molecular Solids: the Partially Oxidized Phthalocyanines," J. Am. Chem. Soc., Vol. 99, p. 286, 1977.

5-3. Ionescu, N. I., and Banyai, P., "Influence of Oxygen on the Dark Conductivity of Copper Phthalocyanine," Rev. Roum. Chim., Vol. 24, pp. 267-70, 1979.

5-4. Kiselev, V. F., Kurylev, V. V., and Levshin, N. L., "The Effect of Adsorption on the Electroconductivity of PcFe and PcCu Films," Phys. Stat. Sol. A, Vol. 42, No. 1, p. K61-4, July 16, 1977.

5-5. Schramm, C. J., Scaringe, R. P., Stojakovic, D. R., Hoffman, B. P., Ibers, J. A., and Marks, T. J., "Chemical, Spectral, Structural, and Charge Transport Properties of the 'Molecular Metals' Produced by Iodination of Nickel Phthalocyanine," J. Am. Chem. Soc., 102, 6702 (1980).

5-6. Sadaoka, Y., Sakai, Y., Yamazoe, N., and Seiyama, T., Chem. Soc. Japan, "Relation between Electrical Conductivity and Thermal Desorption Spectra for the Cobalt Phthalocyanine-Oxidative Gas System," Chem. Lett., Vol. 10, pp. 1263-1266, 1980.

5-7. Marks, T. J., Dirk, C. W., Schoch, Jr., K. F., and Lyding, J. W., "Rational Control of Electronic Structure and Lattice Architecture in Electrically Conducting Molecular/Macromolecular Assemblies," in Molecular Electronic Devices, Forrest L. Carter (ed.), Marcel Dekker, Inc. 1982.

5-8. Bott, B., and Jones, T. A., "A Highly Sensitive NO_2 Sensor Based on Electrical Conductivity Changes in Phthalocyanine Films," Sensors and Actuators, Vol. 5, No. 1, pp. 43-53, January 1984.

5-9. Fan, F. R., and Faulkner, L. R., "Photovoltaic Effects of Metalfree and Zinc Phthalocyanines," J. Chem. Phys., Vol. 69, p. 3334, 1978.

5-10. Vidadi, Y. A., Kocttarli, S., Barkhalov, B. S., and Sadreddinov, S. A., "Direct Current Conductivity of Copper Phthalocyanine Films in the Presence of Blocking Contacts," Phys. Stat. Sol. A, Vol. 33, No. 1, pp. K67-71, January 16, 1976.

TECHNICAL REPORT STANDARD TITLE PAGE

1. Report No. 85-85	2. Government Accession No.	3. Recipient's Catalog No.
4. Title and Subtitle Thin-Film Chemical Sensors Based on Electron Tunneling		5. Report Date November 15, 1986 6. Performing Organization Code
7. Author(s) S.K. Khanna, J. Lambe, H.G. LeDuc, A.P. Thakoor		8. Performing Organization Report No.
9. Performing Organization Name and Address JET PROPULSION LABORATORY California Institute of Technology 4800 Oak Grove Drive Pasadena, California 91109		10. Work Unit No. 11. Contract or Grant No. NAS7-918 13. Type of Report and Period Covered JPL Publication
12. Sponsoring Agency Name and Address NATIONAL AERONAUTICS AND SPACE ADMINISTRATION Washington, D.C. 20546		14. Sponsoring Agency Code

15. Supplementary Notes Sponsored by the U.S. Department of Energy through Interagency Agreement DE-AI01-82ER13007 with NASA; also identified as DOE/ER/13007-1 (RTOP or Customer Code 778-19-75).

16. Abstract

The physical mechanisms underlying a novel chemical sensor based on electron tunneling in metal-insulator-metal (MIM) tunnel junctions were studied. Chemical sensors based on electron tunneling were shown to be sensitive to a variety of substances that include iodine, mercury, bismuth, ethylenedibromide, and ethylenedichloride. A sensitivity of 13 parts per billion of iodine dissolved in hexane was demonstrated. The physical mechanisms involved in the chemical sensitivity of these devices were determined to be the chemical alteration of the surface electronic structure of the top metal electrode in the MIM structure. In addition, electroreflectance spectroscopy (ERS) was studied as a complementary surface-sensitive technique. ERS was shown to be sensitive to both iodine and mercury. Electrolyte electroreflectance and solid-state MIM electroreflectance revealed qualitatively the same chemical response. A modified thin-film structure was also studied in which a chemically active layer was introduced at the top Metal-Insulator interface of the MIM devices. Cobalt phthalocyanine was used for the chemically active layer in this study. Devices modified in this way were shown to be sensitive to iodine and nitrogen dioxide. The chemical sensitivity of the modified structure was due to conductance changes in the active layer.

17. Key Words (Selected by Author(s))	18. Distribution Statement
Conversion Techniques Materials Solid-state Physics	Unclassified-unlimited

19. Security Classif. (of this report)	20. Security Classif. (of this page)	21. No. of Pages	22. Price
Unlimited	Unlimited	42	